Available online at www.sciencedirect.com
SCIENCE DIRECT®
Deep-Sea Research I 51 (2004) 739–753
DEEP-SEA RESEARCH PART I
www.elsevier.com/locate/dsr

Instruments and Methods

Development of a laser Raman spectrometer for deep-ocean science

Peter G. Brewer[a,*], George Malby[a], Jill D. Pasteris[b], Sheri N. White[a], Edward T. Peltzer[a], B. Wopenka[b], J. Freeman[b], Mark O. Brown[a]

[a] *Monterey Bay Aquarium Research Institute, 7700 Sandholdt Road, Moss Landing CA 95039-9644, USA*
[b] *Department of Earth and Planetary Sciences, Washington University, Campus Box 1169, St. Louis, MO 63130-4899, USA*

Received 19 June 2003; received in revised form 26 November 2003; accepted 26 November 2003

Abstract

We have extensively modified and successfully used a laser Raman spectrometer (DORISS, deep-ocean Raman in situ spectrometer) for geochemical studies in the deep ocean. The initial instrument, from Kaiser Optical, was separated into three components: an optical head, a laser-power supply telemetry unit, and the spectrometer. These components were modified to fit into custom designed pressure housings, and connected by deep-sea cables and optical penetrators designed to minimize signal loss. The instrument ensemble has been field deployed on remotely operated vehicles (ROVs) for a variety of experiments and observations, with successful operation at 1.6°C, 3600 m depth. Power supply, instrument control, and signal telemetry are provided through the ROV tether, which contains copper conductors and single mode optical fibers. The optical head is deployable by the ROV robotic arm for sample analysis; the remaining components are fixed within the vehicle tool-sled. Challenges of system calibration at depth, temperature and pressure artifacts, and system control through over 4 km of cable were successfully overcome. We present exemplary spectra obtained in situ of gas, liquid, and solid specimens, and of the ubiquitous signal of sea water itself. Future challenges include weight and size reduction, and advances in precise beam positioning on mineral targets on the sea floor.

Keywords: Laser; Raman spectroscopy; Geochemistry; In situ analysis; Remotely operated vehicle

1. Introduction

Geochemical studies in the deep ocean have traditionally relied upon sample recovery by bottles, cores, and dredges deployed from surface ships, or collected by manned submersibles and remotely operated vehicles (ROVs), to provide specimens for ship or shore based analysis. And while this remains the principal technique, there is a compelling case to be made for advances in in situ detection and analysis. Advances in measurement techniques have been greatly aided by the development and increasing use of deep-ocean submersibles and ROVs. These vehicles now provide sophisticated carrying platforms with the power, telemetry and data handling, and precise manipulation capabilities (Brewer et al., 1999) to support advanced geochemical measurement

*Corresponding author. Tel.: +1-831-775-1706; fax: +1-831-775-1620.
E-mail address: brpe@mbari.org (P.G. Brewer).

0967-0637/$ - see front matter © 2004 Elsevier Ltd. All rights reserved.
doi:10.1016/j.dsr.2003.11.005

systems (Kleinberg et al., 2003). In this paper we describe the adaptation of a laser Raman spectrometer (LRS) for in situ measurements in the deep ocean, and its successful deployment from ROVs operated by the Monterey Bay Aquarium Research Institute (MBARI). In principle the system we describe here could be adapted for use on a variety of ROVs and research submersibles available worldwide. We present exemplary spectra of sea water itself, and of selected geochemical targets examined in a carefully constructed set of controlled field experiments during the development phase, and we briefly describe some important calibration protocols. The verification of these spectra through companion laboratory studies, and detailed discussion of the spectra obtained, is reported by Pasteris et al. (submitted).

A unique advantage of Raman spectroscopy for the field geochemist (Pasteris, 1998) lies in its ability to measure solid, liquid, and gas phases, thereby greatly extending the range of possible targets. The Raman technique can measure very small samples and can provide geochemical traverses across a heterogeneous sample. However, the instrument we describe here has not yet achieved scanning capability.

Sensors typically used (Varney, 2000) for oceanic geochemical research are either electrodes and optrodes, or small-scale pumped fluid devices, for dissolved species detection. These have become sophisticated and are used for mapping geochemical fields and probing seafloor sediment fluids. However, they are typically single species detection systems, not broadly applicable, and the in situ measurement of solid and gaseous phases, has so far not been possible. It is ironic that a prototype Raman spectrometer has been developed for possible exploration of planetary surfaces (Wang et al., 1998, 1999) such as Mars, yet the $>70\%$ of Earth's surface that is ocean has until now not been made accessible to this important tool.

There are many examples of important targets in the deep ocean potentially accessible by Raman spectroscopy. These include the in situ identification of rocks and minerals on the sea floor and the determination of chemical composition of pore water, gas seeps, and sea floor hydrothermal vents. Other interests include biologically (including microbially) precipitated solids such as the polymorphs of elemental sulfur produced by bacteria such as *Thioploca* and *Beggiatoa* (Pasteris et al., 2001). It has been reported that Raman spectroscopy can "characterize in situ the molecular components of pigments and other significant organic and inorganic constituents of a microbial community within its lithic habitat" (Wynn-Williams et al., 2002), although achieving this goal on the ocean floor would seem to be a significant challenge.

It is possible to distinguish between the biologically produced $CaCO_3$ polymorphs aragonite and calcite, and to investigate phosphate minerals and barite deposits on the seafloor. Other Raman active solids of interest on the seafloor include the silicates quartz and feldspar, the iron oxides magnetite and hematite, and the various manganese oxide precipitates. Clathrate hydrate phases (Sloan, 1998; Buffett, 2000; Max, 2000), which incorporate methane and many other gas species into their structure offer a compelling case for measurement in place. These hydrates are not stable at atmospheric pressure and room temperature, but exist in vast quantities in ocean margin sediments where the stability conditions are met. While hydrate specimens may be liberated from the sea floor (Brewer et al., 2002a), they are exceptionally difficult to recover in an unaltered state, and in situ analysis would provide unique information. The Raman spectrum of both CH_4 and CO_2 hydrates has been elegantly investigated in the laboratory (Sum et al., 1997; Subramanian and Sloan, 1999), and in situ analysis would permit the determination of the unaltered state, cage structures, and compositions.

Materials experimentally introduced into the ocean for research purposes may also be Raman active, such as in experiments to investigate the feasibility of fossil fuel CO_2 disposal (Brewer et al., 1999). Finally, possibly toxic material associated with deep ocean waste sites or accidents, where sample recovery may be hazardous, will require non-invasive analysis methods, such as may be provided by laser interrogation.

Nonetheless the challenges of carrying out Raman spectroscopy in the deep ocean are formidable. The Raman signal is notoriously

weak, although possibilities for signal enhancement do exist (e.g. Altkorn et al., 2001). The vast majority of dissolved chemical species in sea water are not Raman active, or are present at micromolar concentrations or less, and thus do not present useful Raman analytes. Water itself has a subdued Raman signature, unlike the overwhelming IR signature of water. Thus the ubiquitous signal of sea water is not likely to produce spectrally complex interferences in the Raman optical path. Fluorescence, on the other hand, is the bane of Raman spectroscopy, and there are many fluorescent oceanic species, including chlorophyll and related pigments. These are abundant in ocean surface waters, but are also rapidly transported to depth by sinking particles. It was unknown at the outset of our work how significant a problem for obtaining oceanic Raman spectra this might be.

Raman instrumentation has been typically fragile, requiring thermal stability, and a vibration free environment. Modern developments in optoelectronics have only now reached the point where these limitations may be overcome. Nonetheless, ships expose the instrumentation to significant physical motions, days of vibration during transit, and physical shock during loading and unloading. Deep ocean water is cold, and during a single lowering to the sea floor the instrumentation may be exposed to temperature changes from 20°C to 2°C in 1 h. The pressure casings that house the instrument must provide protection for a 40 MPa increase in pressure without distorting the encased optical configuration. During expedition work it is very common for instrument reconfiguration to be required, often on a daily basis, and so the system must be capable of open access under often trying field conditions.

Finally, weight and size limitations, power requirements, remote instrument control and positioning, and data telemetry through over 4 km of ROV tether, also provide significant challenges. Signal loss associated with the optical connectors required for pressure housings, and electrical and optical noise that may be introduced by the vehicle, are also issues to be faced. In Fig. 1 we show MBARI's ROV "Tiburon" used for several of our experiments, with the DORISS spectrometer system installed in the vehicle tool sled.

Fig. 1. MBARI's remotely operated vehicle "Tiburon", in side view. The base vehicle weight is 3084 kg. Front, with manipulators and cameras not shown, is to the right of the image. The syntactic foam pack that provides buoyancy is on top, the core vehicle power, thrust, telemetry, and computing, systems are housed in the middle. Below is the tool sled with the drawer used to house the DORISS system seen at bottom left.

2. Experimental

2.1. Selection of an instrument

The research team comprises groups from both MBARI and Washington University, St. Louis. The primary laboratory work was based at Washington University; the primary ocean program was based at MBARI. Each team acquired an initially identical instrument for research compatibility. The MBARI instrument has been very significantly modified in conversion to the

DORISS unit; the Washington University instrument remains in its original configuration. The field experiments for system development were carried out jointly by both teams in the deep waters of Monterey Bay, California.

The DORISS system we have developed is based on a laboratory model laser Raman spectroscopic system from Kaiser Optical Systems, Inc. (KOSI). A schematic diagram of the various components is given in Fig. 2. The requirement for robust handling demanded that the core instrument have as few moving parts as possible, and that the laser give a stable output over a wide temperature range. A frequency-doubled Nd:YAG laser operating at 532 nm was chosen (model DPSS532 by Coherent) because of its stability and its ability to be cooled simply by thermal conduction through the walls of the high-pressure housing. The 532-nm excitation wavelength was selected for its relatively efficient propagation through sea water. The Raman shift is not a function of the exciting wavelength, but the efficiency of Raman scattering from a substance decreases as a function of λ^4, and thus a shorter wavelength laser offers significant advantages. Wavelengths shorter than 532-nm also excite greater fluorescence, and thus the laser selected represents an optimal choice.

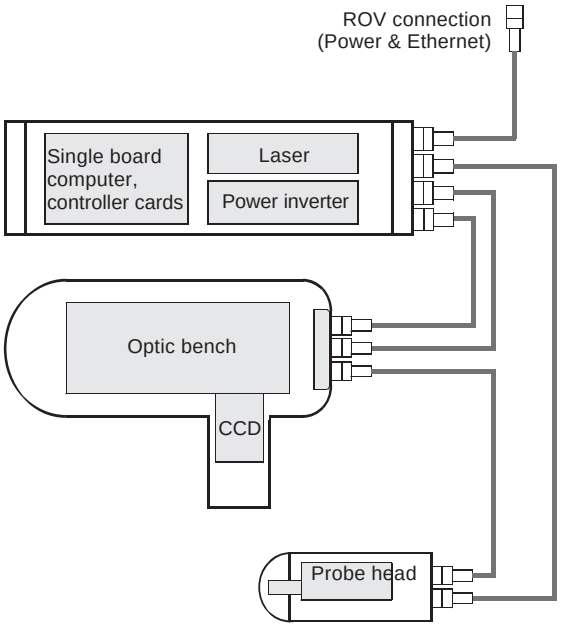

Fig. 2. Schematic of the DORISS system, showing the two pressure housings for the power/laser/computer, and the optical bench. These are carried in the vehicle tool-sled, and are connected to the probe head by pressure tolerant optical fiber cables. The probe head used for sample interrogation is carried on the front of the vehicle so as to be accessible by the vehicle robotic arm.

The requirement for analysis of such a wide range of materials and processes of scientific interest requires a core Raman spectrometer that measures the full spectral range of 100–4000 Δcm^{-1}. The wide spectral coverage is required so that data can be collected in the low-wavenumber range (on sulfur and sulfur containing minerals), mid-range (on most minerals and on volatiles such as CO_2, O_2, N_2), and high range (for organic compounds and for the OH-groups of clathrate hydrates and hydroxylated minerals such as zeolites and clays). Appropriate resolution is required to distinguish mixtures of phases with similar band positions, such as carbonates and experimentally introduced materials with contrasting isotopic shifts (e.g., ^{12}C and ^{13}C).

The selected instrument was a Kaiser HoloSpec f/1.8i spectrometer (Owen et al., 1998) with a holographic transmissive grating and a front-illuminated cooled CCD camera with 2048×512 pixels by Andor Technology. The spectrum is split into two stripes on the face of the camera, thus providing a mapping of 1 cm^{-1} per pixel. This is coupled by fiber optics to Kaiser's Mark II holographic filtered probe head with two interchangeable sampling optics: a "stand-off" optic, and an immersion probe (Fig. 3). We adapted the stand-off optic for housing behind a hemi-spherical deep-sea camera glass dome. It provided a $\sim$10X objective lens with a focal length in air of $\sim$6.4 cm. When immersed in sea water the dome-shielded optic provided a 10 cm working distance for target placement from the outer face of the glass dome. The immersion probe consists of a 2 mm focal length lens integrated into a 25.4 cm long metal tube with a plane sapphire end window and a working distance that is variable over a range of 1–7 mm from the probe tip. The two sampling optics require different pressure housing end caps. The stand-off optic is used by behind the glass dome window (shown assembled in Fig. 3). When the immersion optic is used, the

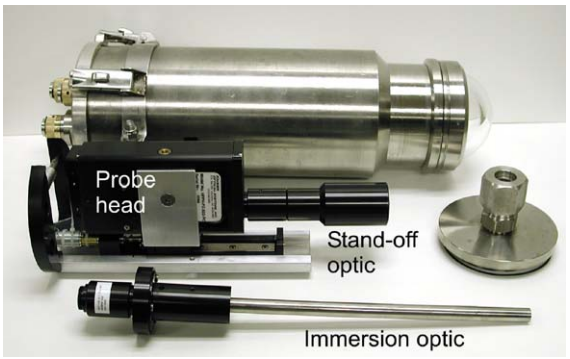

Fig. 3. The probe head, showing the pressure housing (above), and both the stand-off optic, in which the laser beam projects through the glass dome, and the immersion probe with a planar sapphire window at the tip. When the immersion optic is used the dome window is replaced with the flat end cap (seen on the right side of the picture) and a gland seal is used to seal around the probe. We determine ahead of the dive which optic will be appropriate for the target we anticipate. Since the range of focus is far greater for the stand-off optic this offers more flexibility, albeit with somewhat lower sensitivity. The time taken for optic exchange is a few (3–4) h, mostly for fine scale adjustment to achieve maximum laser output.

dome window is replaced by a flat titanium end cap with a gland seal that seals around the protruding optic with the plane sapphire window. The probe extends directly into the water ~20 cm.

2.2. Doriss development

2.2.1. Modification of the original instrument

Communication and control capability for the instrument via Ethernet was added by KOSI at our request at the time of purchase. This is now a standard feature for KOSI instruments. Our need for frequent field adjustment made it necessary to modify two of the original instrument alignment mechanisms. First, the laser-fiber alignment mechanism was replaced with a lockable precision three-axis micrometer stage to facilitate the alignment of the 62.5 μm diameter excitation fiber optic cable to the laser output port. This alignment is critical for delivering and maintaining the maximum laser power to the sample of interest, and correspondingly to obtaining the maximum instrument sensitivity.

Second, the alignment of the lens that focuses the collected Raman signal on the spectrometer slit, which in part determines the spectrometer resolution, is also critical. We found that slight mechanical shock, temperature changes, or orientation deviations could cause the lens-to-slit alignment to shift, degrading the signal. The original KOSI slit alignment mechanism, designed for use in fixed installations on land, used a manual knob to translate the spot across the slit. We have replaced this mechanism with a remotely controllable motor driven stage. The stage translates the scattered-light spot across the slit in 0.5 μm increments. This translation allows a field scientist to optimize the optical throughput of the instrument in real time while at full ocean depth on an individual measurement basis to compensate for changes in the lens/slit alignment that may have occurred during deployment.

2.2.2. Encapsulation

The spectrometer components (schematically shown in Fig. 2) are packaged in three separate pressure vessels capable of withstanding 41 MPa with a 25 percent safety margin. The probe head is contained within a 35.5 cm long by 14 cm diameter titanium pressure vessel (Fig. 3) that has a removable end cap to facilitate the change between different optical configurations. Each probe head configuration weighs 18 kg including supporting frame and manipulator handle. High-pressure tolerant fiber optic cables carry the laser excitation beam to the probe head, and return the Raman scattered signals from the probe head to the spectrometer pressure vessel. The excitation fiber is 62.5 μm diameter; the collection fiber is 100 μm diameter. Signal loss was found to be unacceptably high in standard optical fiber connectors needed to penetrate the pressure housings. The cables we are now using are direct feed-through penetrating cables. These fiber optic cables are standard, pressure-tolerant polyurethane jacketed underwater cables purchased from Falmat, Inc. of San Marcos, CA. Pressure testing performed at MBARI found very small pressure effects on the throughput of the cables.

The electronics (power, telemetry, and laser) pressure vessel (Fig. 4) is 100 cm long, 25.4 cm in

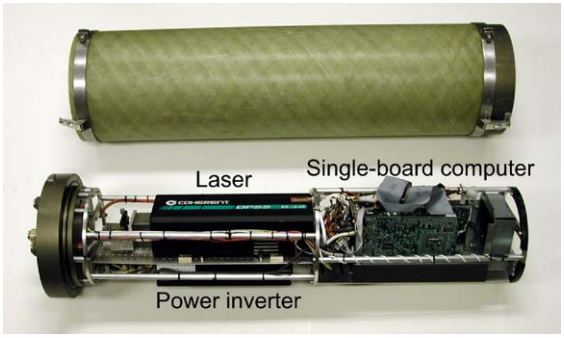

Fig. 4. The fiberglass pressure housing used for the power/laser/computer system, and the incorporated components. The housing is 100 cm long, 25.4 cm diameter.

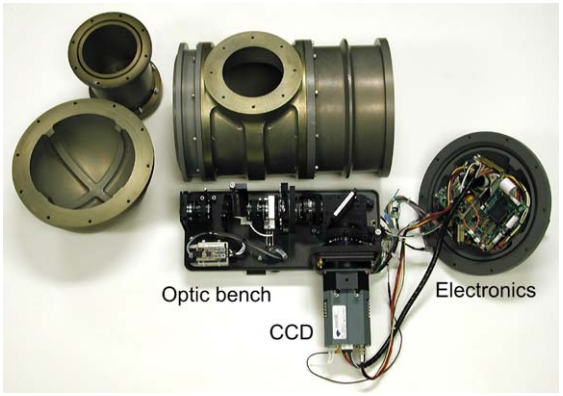

Fig. 5. The pressure housing used to contain the optical bench/spectrometer. The housing end cap incorporates required electronics and the environmental sensors for detecting temperature and humidity.

diameter and weighs 62.6 kg fully assembled. The cylindrical portion of the vessel is a monofilament wound fiberglass reinforced resin 2.5 cm thick lay-up design. 4.4 cm thick removable aluminum end caps complete the assembly. All electronic units are mounted on an internal central aluminum web for support and stabilization. A wheel structure is mounted on each end of the web to position the assembly inside the pressure vessel.

One early design decision was to maintain the original KOSI optical bench layout. While this led to significant design challenges for packaging the system, it enabled us to focus efforts on fielding an instrument rather than on spectrometer redesign. The configuration posed a challenge for pressure vessel design because of the 90° orientation of the charged-coupled device (CCD) camera in relation to the optical components (Fig. 5). Preliminary finite element analysis (FEA) of different designs showed size, weight and applied load to be the main drivers, given the load carrying capacity and space constraints of the ROV. Reviewed options for housing material included Titanium 6AL4V, Stainless 17-4PH, Composite Carbon Fiber and Aluminum 7075. The final selection of Aluminum 7075-T6 was based on its superior properties in yield strength, ease of manufacture, cost, and weight. The final design selection was a unique multi-part assembly that used classic ring stiffened design to provide stiffness for the protruding 90° arm where it intersects the main cylinder body (Fig. 5). The hemispheric end bell provides superior performance at reduced weight as compared to a flat end cap, and also provides space for accommodating essential wiring and components. At the opposite end the truncated hemisphere provides added strength, and a housing surface that can support connector penetrations.

The main body of the housing is 76 cm long, including the hemispherical end caps, and 32 cm diameter. The camera extension is 22 cm long and 20 cm diameter. Total weight of the assembled spectrometer pressure vessel is 78.5 kg. The vessel was machined from 7075 aluminum and has been hard anodized and Teflon impregnated to retard corrosion. The optical bench is held in place inside the pressure vessel by internal jackscrew clamps. Electronic components are mounted both in the hemispherical end cap and under the optical bench.

2.2.3. *Temperature and humidity*

The Raman spectrometer is designed to operate over an ambient temperature range from 0°C to 50°C. Temperature and relative humidity in each of the two major equipment pressure vessels is monitored and the data incorporated into the data stream sent through the single mode fiber of the vehicle umbilical via 10BASE-T Ethernet.

An early design concern was ensuring effective heat transfer from the cooled CCD camera during long dives with high duty cycles, particularly in

warm water masses. Initial heat transfer calculations showed that the densely packed housing provided little air for the fan to move primarily because of the housing design requirement of a 90° extension arm, raising the possibility of sub-optimal operation. The end result of operating in a non-optimal temperature range means increased dark current (essentially leakage of charge into the pixel area that equates to system noise). Dark current is very dependent on temperature and halves in value for approximately every 6°C drop in temperature.

In normal laboratory operation the CCD is cooled to −40°C using an onboard thermoelectric cooling unit and fan; with the addition of water-cooling the array can be cooled to −80°C. A decision was made to design a heat exchanger that would be modular and could be added as necessary for warm water dives. A water-cooled heat transfer assembly was designed into the system that allows for water to circulate to cooling fins, which are external to the housing and cooled by ambient seawater. The water is run in a continuous loop returning to the CCD array at 0.75 l/min. Use of this additional cooling feature has so far not been necessary.

The temperature inside the spectrometer pressure vessel when it is deployed and operating in the deep ocean runs 2–3°C above ambient ocean temperature. At 3600 m depth, 1.6°C, the measured ambient temperature inside the spectrometer pressure vessel was ~4°C. When operating in the laboratory with the spectrometer pressure vessel sealed the inside temperature stabilizes at 5–7°C above room temperature.

The temperature inside the electronics pressure vessel when it is deployed and operating in the ocean stabilizes at 5–10°C above ambient ocean temperature. When operating in the laboratory, with the electronics pressure vessel sealed, the inside temperature stabilizes at 7–13°C above laboratory ambient.

Four or five small packages of desiccant are added to both pressure vessels in preparation for a dive. With the desiccant, the internal relative humidity of both sealed pressure vessels runs at less than 10 percent (at 2°C) of internal vessel temperature and less than 20 percent at 20°C normal laboratory air. All of the above run conditions are well within the manufacturers specifications.

2.2.4. Accommodation on carrying platforms

The accommodation of the DORISS instrument into a vehicle payload poses significant demands. MBARI utilizes two ROVs (www.mbari.org/dmo/vessels/vessels.htm) on which the spectrometer can be deployed to support research in the deep ocean. Each vehicle has a tool-sled with sliders for instrumentation drawers to accommodate the payload (Fig. 1). The ROV Ventana is rated to a depth of 1800 m and has a useful science payload of 272 kg in air. The ROV Tiburon (Fig. 1) is rated to a depth of 4000 m and has a useful science payload of 220 kg in air. Ventana provides 2.5 kW at 120 VAC, and Tiburon provides 200 W at 48 VDC and 5 kW at 240 VDC. Both ROVs provide instrument control through 10BASE-T Ethernet.

The electronics and spectrometer pressure vessels are mounted in an aluminum frame drawer that has a single cable interface to each ROV. The drawer and cabling can be completely installed on or removed from either ROV in less than 30 min. The probe head unit is carried in a location where it may be accessed by the ROV manipulator arm for signal acquisition from the target of interest. The total Raman system weight, including all interconnecting cables and the drawer is 211 kg. Plans to significantly reduce weight are in progress.

2.2.5. Data acquisition and processing

A single board computer, and several PCI expansion cards for remote control of the system, reside in the electronics housing. A standard desktop computer with 10BASE-T Ethernet is used topside to communicate with the single board computer, and to analyze, display and store the spectral data using Kaiser's Holograms software. The data can also be exported to GRAMS, Microsoft Excel, and Matlab software packages for further analysis and manipulation.

2.2.6. Calibration

The DORISS system is calibrated in the lab (ship or shore) prior to each deployment. The calibration is necessary because the system is routinely dismantled and reassembled into its pressure housings for each cruise, causing calibration changes of the instrument. In the present design the CCD camera must be removed from the optic bench when installing the spectrometer in its pressure housing. When the camera is remounted, the pixel positions can shift by as many as 50 pixels from their previous location (in both the vertical and horizontal directions). This is due to tolerances in the camera mounting holes. The calibration kit supplied by Kaiser Optical includes a neon source for wavelength calibration, a tungsten source for intensity calibration, and a cyclohexane standard to verify the laser wavelength (Tedesco and Davis, 1999).

Vibrations and temperature changes can also affect the calibration of the system, typically by a few pixels, which necessitate a calibration reference during deployment. The temperature changes experienced during deployment *differentially* contract the components, and may cause small changes in physical alignment. In order to check this, two in situ calibration routines were devised. Isopropanol contained in a small glass vial with pressure compensation reservoir was carried down with the ROV, and placed in the optical path by the vehicle manipulator whenever a calibration check across the entire CCD detector was desired.

The isopropanol-based calibration method was supplemented by a version of the diamond standard approach of Zheng et al. (2001). A small diamond plate was placed in the beam path within the probe head, but considerably off-focus. This placement moderated the extremely strong scattering efficiency of the diamond, and assured that a weak but readily detectable diamond $1332\,\Delta\mathrm{cm}^{-1}$ band was present in all spectra. The diamond undergoes cooling with the system, but remains at atmospheric pressure. Schiferl et al.(1997) have shown that for changes in temperature of 20–2°C, typical for deep ocean deployment, the diamond band shifts by only $\sim 0.2\,\Delta\mathrm{cm}^{-1}$. Our laboratory tests confirm the modest spectral sensitivity of diamond to temperature changes. Thus this approach provides an effective spectral standard for peak position at all times.

2.3. Remaining technical challenges

There are areas that need improvement, and that are now being addressed. The present procedure uses laser spot positioning by robotic arm placement. This does not enable the precise positioning of the beam required for many operations, and thus spectra of large transparent objects are at present far easier to obtain than those of small opaque objects. Improved laser focusing will be achieved by the addition of a precise positioning unit that can be off-loaded from the vehicle on to the sea floor so as to decouple the probe head from any vehicle motion. This will allow three-dimensional positioning of the laser focal point with high precision on targets of interest.

This first generation DORISS system is sufficiently bulky and heavy that it forms a complete ROV payload, rather than one that would ideally be carried along with other observing tools. This is due in large part to our selection of a standard commercial Raman system for the initial development. The L-configuration of the Kaiser optical bench, with the CCD camera at right angles, is responsible for much of the added size/mass since this dictated the use of a heavy and complex pressure vessel to contain it. In principle significantly smaller designs are possible (Dickensheets et al., 2000; Wang et al., 2003), although their implementation as a deep-sea instrument will pose challenges.

3. Spectral acquisition techniques

We have now used the DORISS system successfully on more than 20 deep-ocean dives, with the emphasis of our efforts being primarily on instrument development. We report here on lessons learned from four in situ case studies, in which we examine materials with known Raman characteristics, and demonstrate successful spectral recovery from the deep ocean. We provide a brief rationale of the criteria for material selection; further

discussion of spectroscopic issues is given in Pasteris et al. (submitted).

3.1. The Raman signal of sea water

The Raman spectrum of sea water is present to some degree in virtually all of our work. Fortunately the spectrum is simple, and easily characterized. Sea water is a solution ($\sim$0.5 M) of 11 "major ions" (present at 1 mg/kg or greater), plus a host of other inorganic and organic species at trace concentrations. Most of the major ionic species are Raman inactive. The pH of sea water varies between 8.3 and 7.6, and it is buffered by a dissolved CO_2 system of about 1.8–2.4 mM. The principal oceanic CO_2 system component is HCO_3^-, and this is only weakly Raman active. The fluorescence of sea water when excited with wavelengths between 350 and 550 nm is well known (Coble, 1996; Chen, 2000), and we had early concerns that this might interfere with the Raman signal. This has not been the case with the 532-nm DORISS system developed here, and all sea water signals recorded below 200 m depth are remarkably free of fluorescence interference.

Raman spectra of sea water acquired in the laboratory, near surface, and at 3600 m depth, are shown in Fig. 6. The Raman spectrum of water has been extensively studied (Walrafen, 1964). Three main modes are designated: the v_1 symmetric (OH) stretch near 3450 Δcm^{-1}, the v_2 H–O–H bending mode near 1640 Δcm^{-1}, and the v_3 water antisymmetric (OH) stretch mode near 3615 Δcm^{-1}. Walrafen (1964) also assigned four additional modes that yield weak Raman signals at 60, 175, 450, and 760 Δcm^{-1} associated with a cluster of a central water molecule surrounded by four hydrogen-bonded water molecules. The Raman spectrum of water is thus well known.

In principle it is possible to determine the concentration of dissolved gases in aqueous solution (Berger et al., 1995) by Raman spectroscopy. The possibility of detecting the dissolved N_2 signal ($\sim$2328 Δcm^{-1}) is small due to both its low concentration and to the fact that N_2 gas in air is present in the probe head as a competing signal. In later experiments we have filled the probe head space with helium to remove this possible ambi-

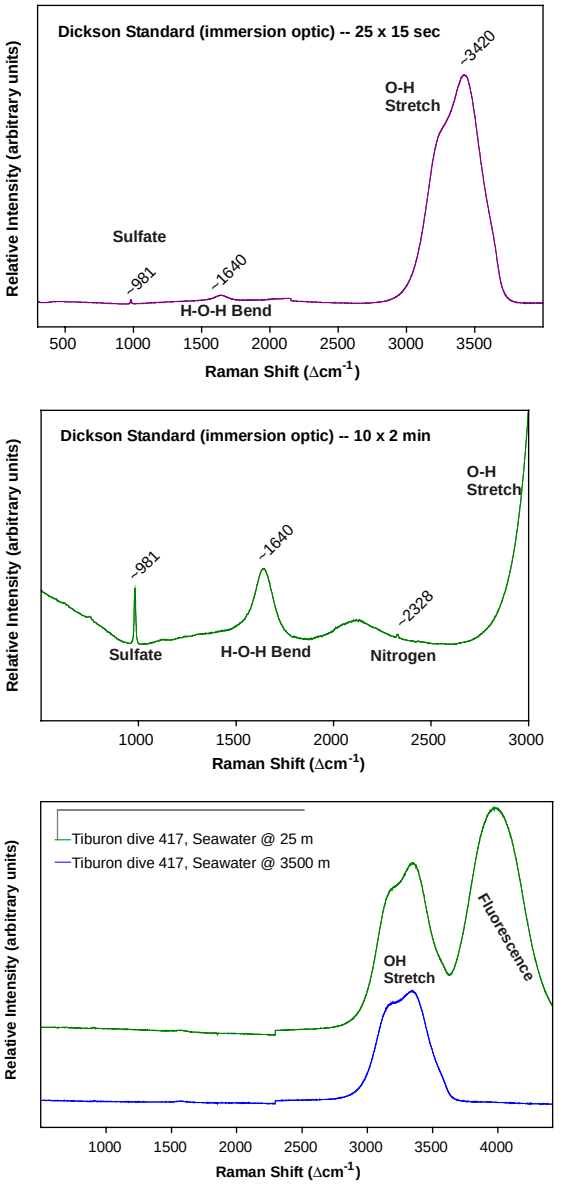

Fig. 6. Comparative spectra of sea water. Upper two panels show spectra of standard sea water (Dickson, 2001) obtained with the immersion optic in the laboratory. The upper panel shows the full spectrum; the center panel focuses on the sulfate and nitrogen peaks. The nitrogen signal has not been corrected for the air contained in the immersion probe itself. The lower panel shows two spectra taken in situ of natural sea water: upper trace from 25 m depth, showing the fluorescence from phytoplankton pigments; and lower trace obtained at 3500 m depth with fluorescence absent.

guity. Both sulfate, and N_2 gas, are conservative properties of sea water and typically show negligible variability. The presence of purely ionic dissolved species (Na^+, Cl^-, Mg^{2+}, etc.) does not yield Raman bands.

The only other obvious signal is that of the S–O stretch ($\sim 981\,\Delta cm^{-1}$) of the sulfate ion. Sulfate is present at 28 mM concentration in sea water of 35 salinity. Since sulfate ion is a conservative component of oxygenated sea water it may well serve as a reliable concentration reference, and as a spectral reference peak. This will be true only if the Raman signal shows no significant dependency on speciation, temperature, and pressure. There is now a very large literature on this point (Appendix) stimulated by questions over the pressure dependence of the anomalous sound absorption of sea water by relaxation of the solvent separated $Mg–H_2O–SO_4$ ion pair. From this literature we can assume that the sea water sulfate Raman signal we observe is indeed a reliable concentration and frequency shift marker. Only very simple applications have so far been made of the field use of the sulfate Raman signal (Murata et al., 1997), such as confirmation of the near-conservative nature of sulfate ion during estuarine mixing.

By contrast the sulfate signal in sediment pore waters can show strong gradients that contain important geochemical information (Borowski et al., 1999), and thus pore waters present important future targets for Raman profiling.

There have been efforts (Abbott et al., 1982; Masutani et al., 1995) to observe the background oceanic CO_2 signal by Raman spectroscopy; all three major dissolved species of the carbonate system (dissolved CO_2, HCO_3^-, and CO_3^{2-}) have Raman active modes, but we have not yet detected these signals in normal ocean waters.

3.2. An ocean Raman gas experiment—N_2+CO_2

One application where no sea water background signal occurs is in the analysis of free gas, in which the immersion probe can be fully surrounded by the phase of interest. Laboratory work has shown that Raman spectroscopy is exceptionally well suited to gas phase analyses of interest to geochemists (Diller and Chang, 1980; Seitz et al., 1993, 1996). Gas vents occur on the sea floor, emitting plumes primarily of methane with traces of higher alkanes, and techniques for their in situ analysis are of interest. Oceanic gas injection of either CO_2 (Haugan and Drange, 1992), or N_2/CO_2 mixtures has been proposed (Saito et al., 2000) as a CO_2 disposal mechanism, where the $\sim$10x higher solubility of CO_2 compared to N_2 in sea water at moderate depth (200–400 m) may be used to effect a separation of the gases so that a dense, sinking CO_2 rich fluid is formed, and the N_2 gas is released. This gas system appeared to offer an *in situ* experiment with a simple optical path with well-known Raman characteristics (Nakamoto, 1997) that was suitable for exploration. In Fig. 7 we illustrate an experiment in which a gas mixture was released into a small box, open to the ocean at the bottom, and with the Raman immersion probe inserted horizontally and penetrating the wall of the box so that the probe tip was fully surrounded by gas. This mimics collection procedures in which gas venting from the sea floor is collected in inverted funnels before transfer to evacuated pressure cylinders for recovery and analysis. A Raman spectrum obtained at 300 m depth is shown in Fig. 8. The simplicity of the

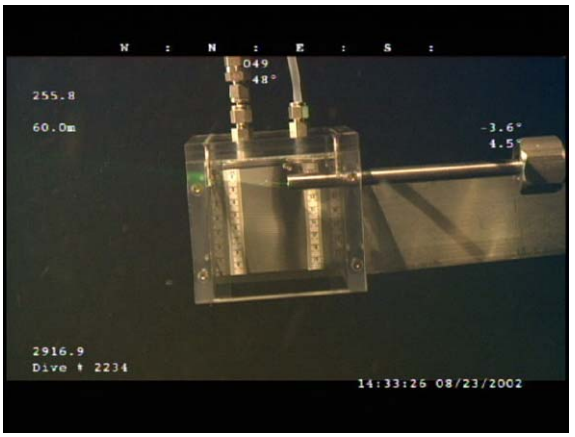

Fig. 7. Image of the in situ gas phase experiment at 255 m depth, showing the immersion probe optic installed in a $10 \times 10 \times 10\,cm^3$ gas cube. The gas handling lines and connectors are visible on top of the cube. In this image the vehicle lights, normally turned off for acquisition of spectra, have been turned on, and the gas is being vented so that the gas/water interface now lies above the probe tip.

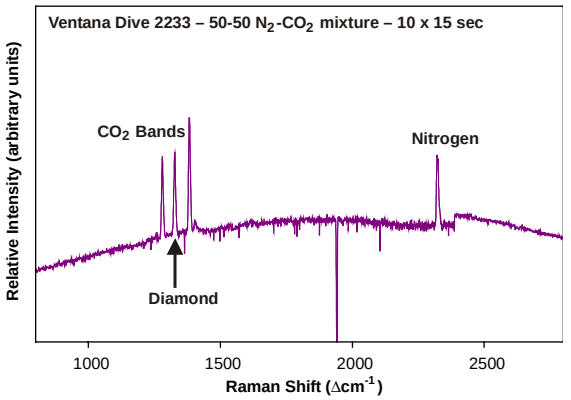

Fig. 8. Spectrum of a 50–50 N_2–CO_2 gas mixture at 300 m depth. The DORISS immersion optic was inserted into a $10 \times 10 \times 10\,cm^3$ bottomless cube (Fig. 7) in which the gas mixture was contained. The diamond reference band ($1332\,\Delta cm^{-1}$) is seen between the Fermi diad of the gaseous CO_2. The signal drop-out at $\sim 1940\,\Delta cm^{-1}$ is due to a flaw on the CCD chip.

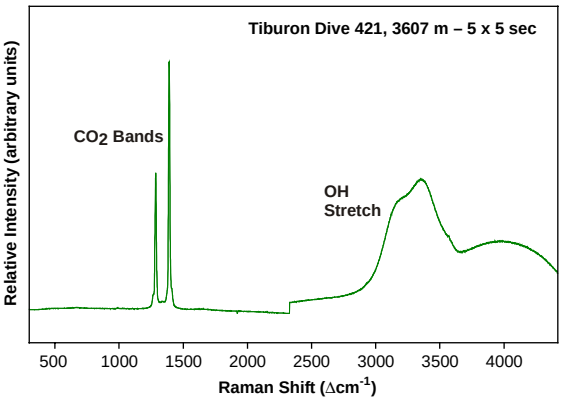

Fig. 9. Raman spectrum of a pool of liquid CO_2 on the sea floor at 3607 m depth, obtained with the stand-off optic. The Fermi diad peaks define the CO_2 signal; the O–H stretch signal results from sea water in the optical path, although not within the focal volume of the lens. The broad hump beyond the O–H stretch band results from fluorescence from organic matter in the surficial marine sediments.

optical path, and the rapid response of the system, indicate that with suitable scaling of gas-liquid ratios it should be possible to quantitatively determine in situ mass transfer coefficients by this method.

3.3. *Liquid phase studies—CO_2*

There are significant vents of fluids into the ocean that provide targets for a Raman spectroscopic probe. For example there are potent fluids at hydrothermal vents and other seeps with potentially very strong Raman signatures. Access to such sites is only available to us on an expeditionary basis, and thus we sought other experimental targets for fluid analysis in order to test the DORISS system.

We have carried out a program to study deep-ocean CO_2 injection techniques for some time now (Brewer et al., 1999, 2002b), and the experimental availability in local waters of this unusual hydrate forming fluid offered a unique opportunity to spectroscopically analyze a non-aqueous liquid on the ocean floor. The relatively large experimental volume and transparent nature of liquid CO_2 provided an operationally easy target for the early stages of development of Raman procedures. We have obtained spectra (Brewer et al., 2002c) of liquid CO_2 on the sea floor (Fig. 9) at 3600 m depth, 1.6°C, during hydrate formation and dissolution rate experiments. We were not yet successful in obtaining unambiguous spectra of CO_2 hydrate, even though it was clearly visible in our experiments. The reason for this appeared to be that the hydrate phase was intermixed with excess liquid CO_2, and that focusing of the beam purely within the relatively thin hydrate film posed operational difficulties. Plans for more precise laser spot positioning and focusing are under development.

The spectrum shown in Fig. 9 reveals only the CO_2 signal, in addition to the bands due to sea water. Equilibrium calculations show that the non-polar nature of liquid CO_2 should result in the strong partitioning of other non-polar compounds (the principal dissolved gases, and some fraction of marine dissolved organic matter) from sea water into the CO_2 phase. We have not yet detected such signals. However equilibrium also dictates that the CO_2 should react with water to form a solid hydrate, and while this has been observed as a rapid reaction (Brewer et al., 1999), the specimen here remained primarily in the liquid state throughout the observing period of several hours.

We predict that the Raman spectrum of CO_2 hydrate formed in natural seawater should reveal signatures of the incorporation of N_2 and O_2 from the dissolved phase, and we plan such experiments.

3.4. Solid mineral Raman signal acquisition—calcite

Raman spectroscopy has the unique advantage of enabling in situ identification of mineral species in the ocean, ranging from filtered suspended particles and hydrothermal precipitates to igneous and sedimentary rocks. However achieving this poses substantial scientific and operational challenges. The principal challenge for our system at this stage of development is the precise and stable location of the laser focal point on a target of interest for the several tens of seconds it takes to acquire a spectrum. We have so far relied upon positioning by vehicle robotic arms, and these are not only insufficiently steady but may also exhibit occasional erratic motions strong enough to break the probe head. Moreover the ROV itself possesses vibrations, and is forced by local ocean velocities, so that maintaining <1 mm positioning precision is unlikely. The need for precise focusing is illustrated by a laboratory study (Fig. 10) in which sampling optics identical to those used for the fieldwork were used to investigate the depth-of-focus in obtaining the Raman spectrum of a silicon wafer. Careful adjustment of the distance between the sampling optics and the opaque sample surface showed the need for position-control to better than 1 mm for the stand-off optic and better than 0.2 mm for the immersion optic in order to acquire a signal at least as strong as one-half the signal at optimum focus. Such precise beam positioning poses challenges for obtaining spectra from opaque targets on the sea floor. This problem is being addressed by the creation of a small off-loadable positioning unit, controllable from the ROV, which will decouple the probe head from vehicle motions and permit precise and steady beam location on targets of interest.

As one example of the potential of this technique we elected to measure a semi-transparent solid, where the strictures on beam positioning are somewhat relaxed. We transported several

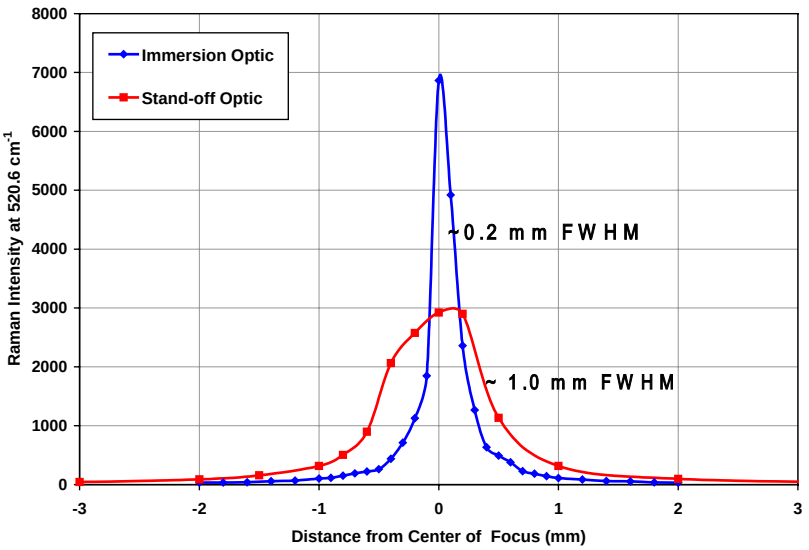

Fig. 10. Example of the beam focusing requirement for an opaque solid for the two probe heads illustrated in Fig. 3. The specimen selected was a silicon wafer. The signal intensity of the $520.6\,\Delta cm^{-1}$ band of silicon was monitored as the probe was moved incrementally closer to the sample, ultimately reaching the optimum focal position (maximum count rate on the Y-axis, 0-point position on the X-axis) and then residing at a distance less than the focal distance. The reported full-width at half-maximum (FWHM) values indicate the range of movement possible in order to still acquire at least half the count rate obtained at the actual focal distance. The results indicate that the immersion optic is much more sensitive to focus than is the stand-off optic.

mineral specimens to 663 m depth, attached to a circular frame that was placed on the sea floor. The stand-off optic configuration was used, and the probe head was placed with the laser beam horizontal and gently adjusted by the vehicle manipulator until the Raman signal was maximized. In Fig. 11 we show the spectrum obtained in situ of a calcite rhomb. There is only a very small sea water contribution to the spectrum obtained (spectral region not shown in Fig. 11). Hydrated and hydroxylated minerals tend to have O–H stretch bands that are much narrower than the O–H stretch from sea water and thus would be readily distinguishable from those of sea water.

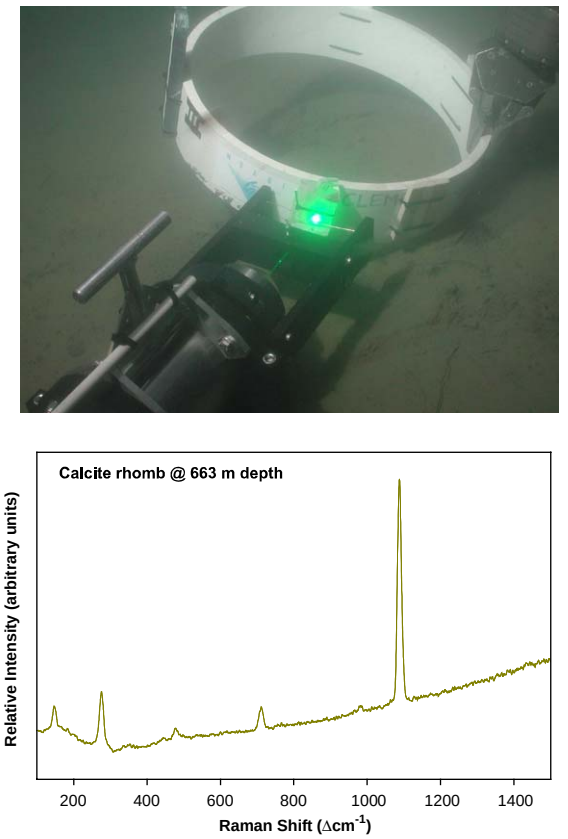

Fig. 11. Upper panel: an image showing ROV arm placement of the DORISS probe head on the sea floor (663 m depth), so as to decouple it from vehicle motions. This allowed adjustment by the vehicle arm to locate the laser focal point within the volume of a rhomb of calcite. The calcite specimen is attached to a circular mount of ~45 cm diameter. Lower panel: the Raman spectrum obtained by the procedure illustrated above.

4. Conclusions

The DORISS system we have described here has successfully obtained high quality Raman spectra in real time from ocean depths down to 3600 m (36 MPa; 1.6°C) from gases, liquids, and mineral solids emplaced in the ocean, and of the signal of sea water itself which permeates our working environment. The integration of remote vehicle operations/ergonomics with Raman techniques is not intuitive, and this has been a significant scientist/engineer/pilot team effort. This essentially completes the testing phase of the system, and application to geochemical problems on an expeditionary basis, and on the essential correlated laboratory studies, is now proceeding.

Finally we note with pleasure that it was an ocean voyage that originally inspired C.V. Raman. A charming account of this is given in his acceptance of the 1930 Nobel prize (Raman, 1930) for physics: "*A voyage to Europe in the summer of 1921 gave me the first opportunity of observing the wonderful blue opalescence of the Mediterranean Sea. It seemed not unlikely that the phenomenon owed its origin to the scattering of sunlight by the molecules of the water.*" Modern optical oceanographers now know far more about this phenomenon, and the anecdote is simply of historical interest. Raman took many sea voyages, and wrote papers while at sea, giving ships and harbors as his address (Venkataraman, 1988). It thus seems fitting that ocean scientists should now seek to take advantage of the remarkable developments in this field.

Acknowledgements

We thank the officers and crew of the RVs Point Lobos and Western Flyer, and the ROV teams of Ventana and Tiburon, for their skill and support at sea. We acknowledge the skilled work of D. Cline in implementing the software for system operation. We thank D. Clague and R. Kleinberg for helpful comments on the manuscript. Funding was provided by a grant to MBARI from the David and Lucile Packard Foundation, and by the US Dept. of Energy Ocean Carbon Sequestration

Program (Grants No. DE-FC26-00NT40929 and DE-FC03-01ER6305).

Appendix

A vigorous debate over sulfate ion association in sea water was stimulated by the claim by Kester and Pytkowicz (1970) that the anomalous sound absorption due to relaxation of the $Mg–H_2O–SO_4$ pair should increase with depth. This was followed by a Raman spectroscopic study (Daly et al., 1972) that purported to support this model. The basis for this experimental attack is that aqueous $MgSO_4$ solutions of $\sim 0.5\,M$ at room temperature show the strong ν_1 stretching band at $981\,\Delta cm^{-1}$, and a weak shoulder on the peak at around $995\,\Delta cm^{-1}$ resulting from $Mg–SO_4$ ionic interaction, which thus yields a slight asymmetry to the profile. Davis and Oliver (1973) challenged the work of Daly et al. (1972), and reported that "it is not possible to distinguish the two types of solvent separated ion pairs from each other, or the sulfate in solvent separated ion pairs from the solvated sulfate ion." Further high-pressure work by Chatterjee et al. (1974) supported the conclusions of Davis and Oliver (1973). This rebuttal of the claims of Kester and Pytkowicz (1970) was strongly supported by Fisher (1978). Recent work (Rull and Sobron, 1994; Frantz et al., 1994) confirms by both experiment and models that such weak pairing is reflected only as a shoulder on the principal peak, and that this is only detectable at high solution strengths, and at temperatures higher than the deep ocean. We therefore conclude that the small fraction ($\sim 4\%$) of $Mg–SO_4$ contact ion pairs in sea water, does not affect our observed signal.

References

Abbott, T., Buchanan, G.W., Kruus, P., Lee, K.C., 1982. ^{13}C Nuclear magnetic resonance and Raman investigations of aqueous carbon dioxide systems. Canadian Journal of Chemistry 60, 1000–1006.

Altkorn, R., Malinsky, M.D., Van Duyne, R.P., Koev, I., 2001. Intensity considerations in liquid core optical fiber Raman spectroscopy. Applied Spectroscopy 55, 373–381.

Berger, A.J., Wang, Y., Sammeth, D.M., Itzkan, I., Kneipp, K., Feld, M.S., 1995. Aqueous dissolved-gas measurements using near-infrared Raman spectroscopy. Applied Spectroscopy 49, 1164–1169.

Borowski, W.S., Paull, C.K., Ussler, W., 1999. Global and local variations of interstitial sulfate gradients in deep-water, continental margin sediments: sensitivity to underlying methane and gas hydrates. Marine Geology 159, 131–154.

Brewer, P.G., Friederich, G., Peltzer, E.T., Orr Jr., F.M., 1999. Direct experiments on the ocean disposal of fossil fuel CO_2. Science 284, 943–945.

Brewer, P.G., Paull, C., Peltzer, E.T., Ussler, W., Rehder, G., Friederich, G., 2002a. Measurements of the fate of gas hydrates during transit through the ocean water column. Geophysical Research Letters 29, doi: 10.1029/2002GL014727.

Brewer, P.G., Peltzer, E.T., Friederich, G., Rehder, G., 2002b. Experimental determination of the fate of rising CO_2 droplets in seawater. Environmental Science and Technology 36, 5441–5446.

Brewer, P.G., Pasteris, J., Malby, G., Peltzer, E.T., White, S., Freeman, J., Wopenka, B., Brown, M., Cline, D., 2002c. Laser Raman spectroscopy used to study the ocean at 3600-m depth. EOS, Transactions, American Geophysical Union 83, 469–470.

Buffett, B.A., 2000. Clathrate hydrates. Annual Review of Earth and Planetary Sciences 28, 477–507.

Chatterjee, R.M., Adams, W.A., Davis, A.R., 1974. A high-pressure laser Raman spectroscopic investigation of aqueous magnesium sulfate solutions. The Journal of Physical Chemistry 78, 246–250.

Chen, R.F., 2000. A laser-based fiber-optic fluorometer for in situ seawater measurements. In: Varney, M.S. (Ed.), Chemical sensors in oceanography. Gordon and Breach, London, pp. 189–209.

Coble, P.G., 1996. Characterization of marine and terrestrial DOM in sea water by rising excitation-emission spectroscopy. Marine Chemistry 51, 325–346.

Daly, F.P., Brown, C.W., Kester, D.R., 1972. Sodium and magnesium sulfate ion pairing: evidence from Raman spectroscopy. The Journal of Physical Chemistry 76, 3664–3668.

Davis, A.R., Oliver, B.G., 1973. Raman spectroscopic evidence for contact ion pairing in aqueous magnesium sulfate solutions. The Journal of Physical Chemistry 77, 1315–1316.

Dickensheets, D.L., Wynn-Williams, D.D., Edwards, H.G.M., Schoen, C., Crowder, C., Newton, E.M., 2000. A novel miniature confocal microscope/Raman spectrometer system for biomolecular analysis on future Mars missions after Antarctic trials. Journal of Raman Spectroscopy 31, 633–635.

Dickson, A., 2001. Reference materials for oceanic measurements. Oceanography 14 (4), 21–22.

Diller, D.E., Chang, R.F., 1980. Composition of mixtures of natural gas conponents determined by Raman spectrometry. Applied Spectroscopy 34, 411–414.

Fisher, F., 1978. Comment on "a high-pressure laser Raman spectroscopic investigation of aqueous magnesium sulfate solutions". The Journal of Physical Chemistry 82, 495–496.

Frantz, J.D., Dubessy, J., Mysen, B.O., 1994. Ion-pairing in aqueous $MgSO_4$ solutions along an isochore to 500°C and 11 kbar using Raman spectroscopy in conjunction with the diamond-anvil cell. Chemical Geology 116, 181–188.

Haugan, P.M., Drange, H., 1992. Sequestration of CO_2 in the deep ocean by shallow injection. Nature 357, 318–320.

Kester, D.R., Pytkowicz, R.M., 1970. Effect of temperature and pressure on sulfate ion association in sea water. Geochimica et Cosmochimica Acta 34, 1039–1051.

Kleinberg, R.L., Flaum, C., Straley, C., Brewer, P.G., Malby, G.E., Peltzer, E.T., Friederich, G., Yesinowski, J.P., 2003. Seafloor nuclear magnetic resonance assay of methane hydrate in sediment and rock. Journal of Geophysical Research 108, doi:10.1029/2001JB000919.

Masutani, S.M., Kinoshita, C.M., Nihous, G.C., Teng, H., Vega, L.A., Sharma, S.K., 1995. Laboratory experiments of CO_2 injection into the ocean. In: Handa, N., Ohsumi, T. (Eds.), Direct Ocean Disposal of Carbon dioxide. Terra Scientific Publishing, Tokyo, pp. 239–252.

Max, M.D., 2000. Natural Gas Hydrate in Oceanic and Permafrost Environments. Kluwer, Academic Publishers, Dordrecht, 414 pp.

Murata, K., Kawakami, K., Matsunaga, Y., Yamashita, S., 1997. Determination of sulfate in brackish waters by laser Raman spectroscopy. Analytica Chimica Acta 344, 153–157.

Nakamoto, K., 1997. Infrared and Raman Spectra of Inorganic and Coordination Compounds. Part A: Theory and Applications in Inorganic Chemistry. Wiley, New York, 387 pp.

Owen, H., Battery, D.E., Pelletier, M.J., Slater, J., 1998. New spectroscopic instrument based on volume holographic optical elements. Proceedings SPIE 2406, 260.

Pasteris, J., 1998. The laser Raman microprobe as a tool for the economic geologist. In: McKibben, M.A., Shanks, W.C., Ridley, W.I. (Eds.), Applications of microanalytical techniques to understanding mineralizing processes. Society of Economic Geologists, Littleton, CO, pp. 233–250.

Pasteris, J.D., Freeman, J.J., Goffredi, S.K., Buck, K.R., 2001. Raman spectroscopic and laser scanning confocal microscopic analysis of sulfur-precipitating marine bacteria. Chemical Geology 180, 3–18.

Pasteris, J.D., Wopenka, B., Freeman, J.J., Brewer, P.G., White, S.N., Peltzer, E.T., George, E., Malby, G.E., Spectroscopic successes and challenges: Raman spectroscopy at 3.6 Km depth in the ocean. Applied Spectroscopy, in review.

Raman, C.V., 1930. The molecular scattering of light. Nobel Prize Lecture.

Rull, F., Sobron, F., 1994. Band profile analysis of the Raman spectra of sulfate ions in aqueous solutions. Journal of Raman Spectroscopy 25, 693–698.

Saito, T., Kajishima, T., Naguosa, R., 2000. CO_2 sequestration at sea by gas-lift system of shallow injection and deep releasing. Environmental Science and Technology 34, 4140–4145.

Schiferl, D., Nicol, M., Zaug, J.M., Sharma, S.K., Cooney, T.F., Wang, S.Y., Anthony, T.R., Fleischer, J.F, 1997. The diamond $^{13}C/^{12}C$ isotope Raman pressure sensor system for high-temperature/pressure diamond-anvil cells with reactive samples. Journal of Applied Physics 82, 3256–3265.

Seitz, J.C., Pasteris, J.D., Chou, I.-M., 1993. Raman spectroscopic characterization of gas mixtures. I. Quantitative composition and pressure determinations of CH_4, N_2, and their mixtures. American Journal of Science 293, 297–321.

Seitz, J.C., Pasteris, J.D., Chou, I.-M., 1996. Raman spectroscopic characterization of gas mixtures. II. Quantitative composition and pressure determination of the CO_2–CH_4 system. American Journal of Science 296, 577–600.

Sloan, E.D., 1998. Clathrate Hydrates of Natural Gases. Marcel Dekker, New York, 705 pp.

Subramanian, S., Sloan Jr., E.D., 1999. Molecular measurements of methane hydrate formation. Fluid Phase Equilibria, 158–160, 813–820.

Sum, A.K., Burruss, R.C., Sloan Jr., E.D., 1997. Measurement of clathrate hydrates via Raman spectroscopy. Journal of Physical Chemistry 101, 7371–7377.

Tedesco, J.M., Davis, K.L., 1999. Calibration of dispersive Raman process analyzers. Proceedings of SPIE, 3537 200–212.

Varney, M.S. (Ed.), 2000. Chemical Sensors in Oceanography, Gordon and Breach, The Netherlands, p. 333.

Venkataraman, G., 1988. Journey into Light: Life and Science of C.V. Raman. Indian Academy of Sciences.

Walrafen, G.E., 1964. Raman spectral studies of water structure. The Journal of Chemical Physics 40, 3249–3256.

Wang, A., Haskin, L.A., Cortez, E., 1998. Prototype Raman Spectroscopic sensor for in situ mineral characterization on planetary surfaces. Applied Spectroscopy 52, 477–487.

Wang, A., Jolliff, B.J., Haskin, L.A., 1999. Raman spectroscopic characterization of a highly weathered basalt: igneous mineralogy, alteration products, and a microorganism. Journal of Geophysical Research 104, 27067–27077.

Wang, A., Haskin, L.A., Lane, A.L., Wdowiak, T.J., Squyres, S.W., Wilson, R.J., Hovland, L.E., Manatt, K.S., Raouf, N., Smith, C.D., 2003. Development of the Mars microbeam Raman spectrometer (MMRS). Journal of Geophysical Research 108, doi: 10.1029/2002JE001902.

Wynn-Williams, D.D., Edwards, H.G.M., Newton, E.M., Holder, J.M., 2002. Pigmentation as a survival strategy for ancient and modern photosynthetic microbes under high ultraviolet stress on planetary surfaces. International Journal of Astrobiology 1, 39–49.

Zheng, X., Fu, W., Albin, S., Wise, K.L., A. Javey, K.L., Cooper, J.B., 2001. Self-referencing Raman probes for quantitative analysis. Applied Spectroscopy 55, 382–388.